In summary, we have observed and explained broad short-wave radiation under well-defined experimental conditions. In our experiments, self-phase modulation is negligible and self-focusing is absent. It is expected—and preliminary experiments confirm—that the same physical mechanism contributes to superbroadening also in other materials under more complex experimental conditions.[4]

[1]M. D. Levenson, C. Flytzanis, and N. Bloembergen, Phys. Rev. B 6, 3962 (1972); J. J. Wynne and J. R. Lankard, Appl. Phys. Lett. 29, 650 (1972).

[2]P. P. Sorokin, J. J. Wynne, and J. R. Lankard, Appl. Phys. Lett. 22, 342 (1973).

[3]Noncollinear phase-matched four-photon interaction has been reported in self-focused beams by R. R. Alfano and S. L. Shapiro, Phys. Rev. Lett. 24, 584 (1970).

[4]For references see S. A. Akhmanov, R. V. Khokhlov, and A. P. Sukhorukov, in Laser Handbook, edited by F. T. Arecchi and E. O. Schulz DuBois (North-Holland, Amsterdam, 1972).

[5]D. L. Weinberg, Appl. Phys. Lett. 14, 32 (1969); W. Werncke, A. Lau, M. Pfeiffer, K. Lenz, H.-J. Weigmann, and C. D. Thuy, Opt. Commun. 4, 413 (1972); V. S. Dneprovsky, K. V. Karmenjan, and I. I. Nurminsky, Izv. Akad. Nauk Arm. SSR, Fiz. 7, 348 (1972).

[6]O. Rahn, M. Maier, and W. Kaiser, Opt. Commun. 1, 109 (1969); G. E. Walrafen, J. Chem. Phys. 47, 114 (1967), and private communication.

[7]M. Paillette, Ann. Phys. (Paris) 4, 671 (1969).

[8]R. R. Alfano, L. L. Hope, and S. L. Shapiro, Phys. Rev. A 6, 433 (1972).

[9]D. von der Linde, IEEE J. Quant. Electron. 8, 328 (1972).

[10]As a guide for deriving Eq. (1) see A. Yariv and J. E. Paerson, in Progress in Optics, edited by J. H. Sanders and K. W. H. Stevens (Pergamon, New York, 1969), Vol. 1.

[11]For a discussion of the initial conditions see Ref. 10, and A. Yariv, Quantum Electronics (Wiley, New York, 1968).

[12]E. K. Plyler and N. Acquista, J. Opt. Soc. Amer. 44, 505 (1954).

[13]The group-velocity dispersion allows an interaction between pump $\tilde{\nu}_L$ and signal $\tilde{\nu}_3$ for more than 4 cm.

[14]J. A. Armstrong, N. Bloembergen, J. Ducuing, and P. S. Pershan, Phys. Rev. 127, 1918 (1962).

[15]R. W. Terhune and P. D. Maker, in Lasers, edited by A. K. Levine (Marcel Dekker, New York, 1968), Vol. 2.

[16]This assumption may be justified as follows: $\langle c_i | x^3 | g \rangle = \sum_j \langle c_i | x | a_j \rangle \langle a_j | x^2 | g \rangle \simeq \sum_l \langle c_i | x | a_l \rangle \langle a_l | x^2 | g \rangle = \langle c_i | x | \overline{a} \rangle \times \sum_l \langle a_l | x^2 | g \rangle = \langle c_i | x | \overline{a} \rangle C_1 \simeq \langle c_i | x | g \rangle C_2$, C_1 and C_2 being constants. The first sum runs over all states $| a_j \rangle$ with the same parity as $| g \rangle$ (other matrix elements are zero). In the second sum only the states $| a_l \rangle$ are retained which form large matrix elements. These states $| a_l \rangle$ have a shape similar to $| g \rangle$. This fact implies that $| \overline{a} \rangle$ is similar to $| g \rangle$ in the averaged matrix element $\langle c_i | x | \overline{a} \rangle$ and that $\langle c_i | x | \overline{a} \rangle \simeq \text{const} \times \langle c_i | x | g \rangle$.

[17]Preliminary calculations show that frequency conversion, $\omega_L + \omega_L + \omega_4 \rightarrow \omega_3$, contributes at high laser intensities.

Excitation of Quasicylindrical Waves Connected with Electron Bernstein Modes

A. Gonfalone

Space Science Department, European Space Research Organization, Noordwijk, Holland

and

C. Beghin

Groupe de Recherches Ionisphériques, Centre National de la Recherche Scientifique, 45045 Orléans, France

By measuring the potential around a point-source antenna in a high-density magnetoplasma at a frequency between the electron gyrofrequency and the plasma frequency, we have detected an interference between a slow electrostatic wave and the cold plasma field. A model of quasicylindrical electrostatic waves connected with the Bernstein mode is proposed to explain the results.

We have measured the potential around a small antenna embedded in a magnetoplasma. According to cold-plasma theory, the potential is maximum on a cone with its apex at the source and its axis along the magnetic field when the frequency is either in the range of the upper oblique resonance (ω between the plasma frequency ω_p, or the gyrofrequency ω_c if $\omega_c < \omega_p$, and the upper-hybrid frequency) or in the range of the lower oblique resonances ($\omega < \omega_c$ or ω_p if $\omega_c > \omega_p$).

These oblique resonances have been observed in laboratory plasmas by Fisher and Gould[1] and Gonfalone,[2] and in space with a satellite experiment by McPherson et al.[3] These resonance curves for the upper and the lower branches observed in our laboratory are shown in Figs. 1(a)–1(c). The fine structure, observed inside the cone for the lower branch [Figs. 1(a) and 1(c)] and outside the cone for the upper branch [Fig. 1(b)] has been interpreted[1] as interference between the fast electromagnetic wave and a slow plasma wave.

In this paper we present and discuss a new propagation mode, observed in a frequency range where neither an electromagnetic wave nor an oblique resonance exists. In this instance, the fine structure appears almost everywhere around the source [Fig. 1(d)] and is interpreted as interference between the static cold plasma field and a quasicylindrical electrostatic wave which is connected with the lowest-order Bernstein mode[4] in perpendicular propagation.
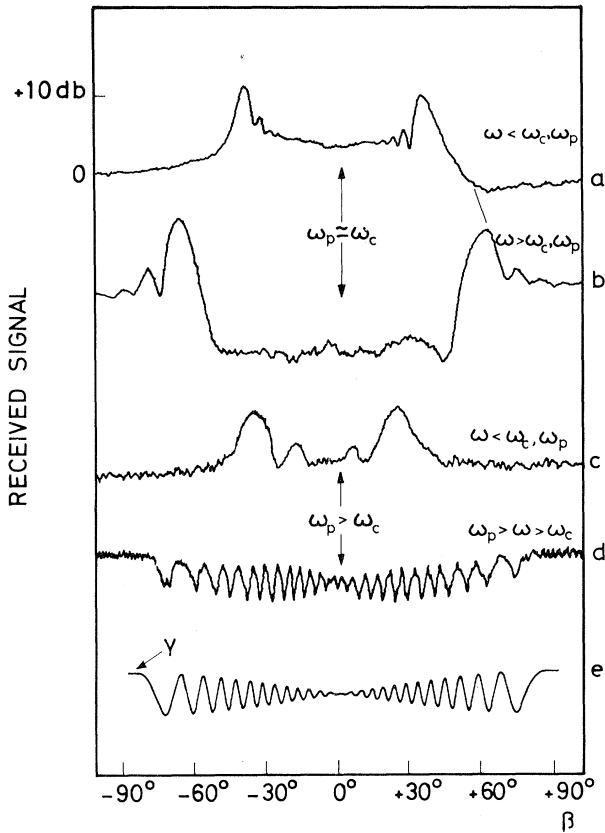
FIG. 1. (a)–(d) Potential of the reception antenna (log scale) as a function of β (angle between antennas and magnetic field). (e) Theoretical curve according to the cylindrical-wave model.

A description of the experimental setup is given in Ref. 2. The curves in Fig. 1 have been obtained in the following manner. A repetitive voltage pulse applied between an anode and a hot cathode produces an afterglow plasma in a cylindrical vessel, and a uniform magnetic field $\vec{B}_0$ is directed along its axis. The central conductor of a coaxial cable exposed over a length of 5 mm is used as the radiating part of the transmitting antenna, and a similar antenna is used for the reception. The two antennas are 10 cm apart and rotate around an axis perpendicular to the magnetic field. A network analyzer is then used to obtain the envelope of the received signal as a function of the angle β between the magnetic field and the line joining the antennas.

To explain the reception of slow electrostatic waves whose arrival directions are very oblique with respect to the magnetic field and whose frequency range is one forbidden to oblique resonances, we have studied the solution of the dispersion equation in a warm magnetoplasma in accordance with classical theory (Boltzmann's and Maxwell's equations), but with the electrostatic approximation.

If an isotropic electron temperature is assumed $(T_\parallel = T_\perp = T)$ and the effect of ions is neglected, this equation is as follows[5]:

$$1 + (\omega_p^2/\omega_c^2)[\sin^2(\theta)/\lambda]$$

$$\times[1 + i\alpha_0 e^{-\lambda}\sum_{-\infty}^{+\infty} I_n(\lambda)F_0(\alpha_n)] = 0, \qquad (1)$$

where

$$\lambda = k_\perp^2\rho^2 = (k_\perp^2/\omega_c^2)KT/m,$$

$$\alpha_n = [(\omega + n\omega_c)/k_\parallel](m/2KT)^{1/2},$$

$$F_0(\tau) = \sqrt{\pi}[\mathrm{Re}(k_\parallel)/|\mathrm{Re}(k_\parallel)|]\exp(-\alpha_n^2) + 2iS(z),$$

$$S(z) = e^{-z^2}\int_0^z e^{t^2}dt,$$

θ is the angle between $\vec{k}$ and $\vec{B}_0$ (not to be confused with β), ρ is the electron Larmor radius, and $\mathrm{Re}(k_\parallel)$ is the real part of $k_\parallel$.

Equation (1) has been solved numerically by many authors, especially for $\theta = \pi/2$, in which case the solution is simplified and gives the well-known Bernstein modes.[4] Generally Eq. (1) must be solved in the complex eight-dimensional space $(\omega, \vec{k})$, and this makes representation of solutions (usually damped or unstable waves) very complicated. Furthermore, Eq. (1), including multivalued functions, has an infinite number of solutions. All the solutions which have been studied to date
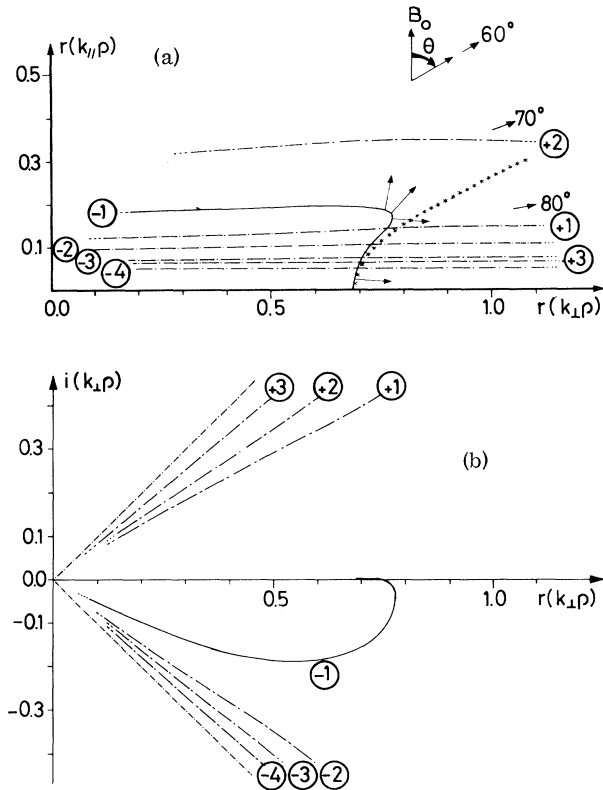
FIG. 2. (a) Projection in the real plane of index surfaces of the first branches of microscopic solutions for $\omega/\omega_c = 1.5$ and $\omega_p^2/\omega_c^2 = 3$. Asterisks, full-adiabatic solution. (b) Projection in the complex plane of the same branches.

can be classified into three different groups: (i) $\vec{k}$ real and ω complex; see, e.g., Tataronis and Crawford[6]; (ii) $k_\parallel$ and ω real, $k_\perp$ complex (e.g., θ complex); see Trulsen[7]; (iii) ω real and $\vec{k}$ complex (θ real); see Oya.[8]

Here the last representation is adopted because it is well adapted to the experimental situation where the potential around the point source has to be computed. Because of the symmetry around the magnetic field, the complex domain of $\vec{k}$ can be reduced to $k_\parallel$ and $k_\perp$; and, letting θ be real, the components of $\vec{k}$ obey the following relation:

$$\tan\theta = \frac{k_\perp}{k_\parallel} = \frac{\mathrm{Im}(k_\perp)}{\mathrm{Im}(k_\parallel)} = \frac{\mathrm{Re}(k_\perp)}{\mathrm{Re}(k_\parallel)} = \frac{|k_\perp|}{|k_\parallel|},$$

Consequently, the solutions of Eq. (1) can be studied in three-dimensional space when ω is kept constant; the coordinates will then be $\mathrm{Re}(k_\perp\rho)$, $\mathrm{Im}(k_\perp\rho)$, and $\mathrm{Re}\,(k_\parallel\rho)$. The different solutions are presented in Figs. 2(a) and 2(b). Each branch represents a solution and is given an arbitrary

identification index whose sign is that of $\mathrm{Im}(k_\perp\rho)$. The fact that the two signs may coexist for waves which are always subject to damping, in a Maxwellian plasma, has been discussed by Oya,[8] and he has indicated that the energy of the two types of waves propagates in opposite directions. Figures 2(a) and 2(b) show that the dominant pole is the branch (-1), which is the classical Bernstein's mode. All the other branches, representing strongly damped waves, are close to the two bisectors and correspond to a damping of more than 50 dB over a wavelength. The (-1) branch is highly damped only after the kink, which appears in the real plane [Fig. 2(a)]. The interesting part of this branch therefore lies between $\theta = \pi/2$ and the kink at $\theta \sim 75°$. In this part, because of the relatively small damping, progressive waves can exist and, in particular, the concepts of wave surface and direction of propagation can be used. The remarkable peculiarity of this mode is that although the wave vector $\vec{k}$ deviates only by a few degrees from $\theta = \pi/2$, the direction of propagation of energy shown by arrows in Fig. 2(a) covers practically the whole space. Besides, $|\vec{k}|$ remains nearly constant (only a few percent change), and the electrostatic field produced by a point source is in phase on quasicylindrical surfaces with the steady magnetic field along the symmetry axis.

The dominant branches of the solutions for three values of the ratio ω/ω_c are plotted in Fig. 3 in the same space as in Fig. 2, but with a perspective representation that offers three advantages: (a) It gives a total picture of the solutions in the complex space; (b) the vertical view is the usual diagram for the index surface in polar coordinates; (c) the horizontal view gives the degree of damping of the wave.

In the scope of the experiment described here, the potential could be theoretically computed by using Fourier-Laplace transforms. It would then be necessary to integrate Poisson's equation in the complex space around all the poles of Eq. (1), but this calculus is not the purpose of the paper and would constitute a further step. Nevertheless, it can be anticipated that the potential at a given point will be mainly the sum of the two main poles: the pole of the cold-plasma theory (or vacuum pole $\vec{k} = 0$), which always appears in the integration of Poisson's equation, and the electrostatic-wave dominant pole in the range where damping can be neglected. Because of the principle of the stationary phase, this electrostatic pole will be practically limited to the point
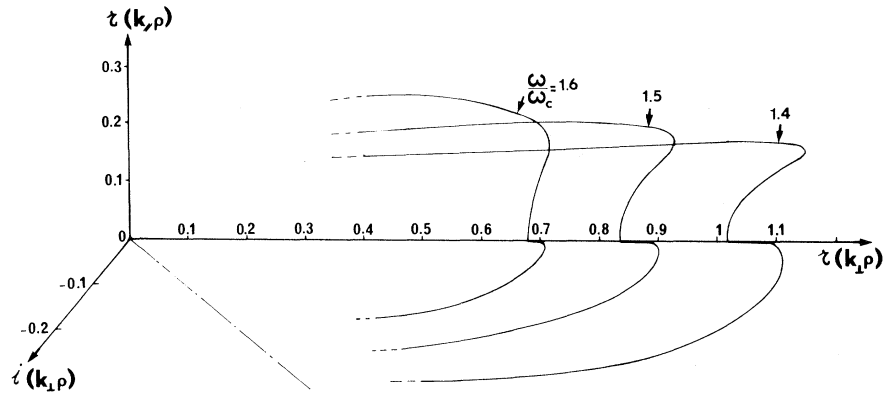
FIG. 3. Complex representation of dominant branches for different frequencies and for $\omega_p^2/\omega_c^2 = 5$.

of the index surfaces lying between $\theta = \pi/2$ and the kink where the energy propagates in the direction of the receiving antenna. This preliminary analysis explains the observation of interferences, in practically the whole space, between the cold plasma field and the field of the slow electrostatic wave whose wave vector, almost transverse, is very close to the solution of the Bernstein mode for $k_{\parallel} = 0$.

Because of the actual shape of the index surface, there should be one, two, or three interfering electrostatic waves from the same dominant branch with different wave vectors $\vec{k}$ and the same energy direction, but because their wavelengths are close together, at short distances from the source, their field interfering with the cold plasma field should be coherent. Anticipating the exact result from the integration mentioned above, we shall consider as a first approximation that the equipotential surfaces are cylinders around $\vec{B}_0$, so that the interference pattern around the transmitting antenna has the following form:

$$y' = \cos(k_\perp d \sin\beta + \varphi_0),$$

where d is the distance between the antennas, and φ_0 the phase shift between the electrostatic wave and the cold static field at the source. Taking into account the amplitude variation of the experimental signal, the function y' has been multiplied by an empirical factor $\sin\beta$. This factor allows a better comparison between the experimental and the theoretical curves, but gives no new information on the structure of the wave. Figure 1(e) shows that the function

$$y = \sin\beta \, \cos(k_\perp d \sin\beta + \varphi_0)$$

agrees well with the experimental curve. This

agreement thus confirms the model of cylindrical waves. As the distance d is known, $k_\perp$ can be accurately deduced. A series of curves similar to that in Fig. 1(d) has been obtained by changing the emission frequency. The different wave numbers are plotted against frequency in Fig. 4. The solid line is the theoretical curve deduced from the dispersion equation of the Bernstein mode which fits the experimental points best, the Lar-
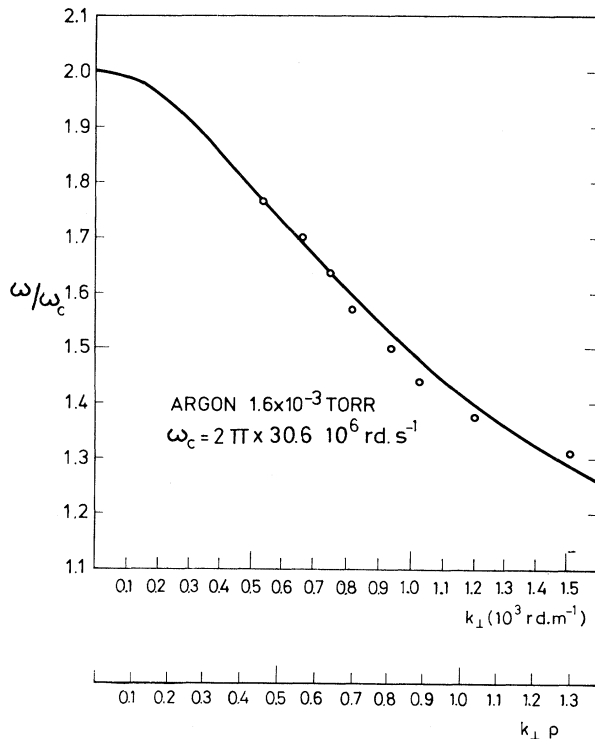
FIG. 4. Wave number $k_\perp$ as a function of frequency, experimental points and theoretical curve. Lower scale, Bernstein dispersion curve for $\omega_p^2/\omega_c^2 = 5$; the comparison of the two scales gives $T = 1800°$K.

mor radius ρ being unknown. In the experimental setup there is no independent method for measuring the density, but the temperature measured with an electrostatic probe compares favorably with the value deduced from Fig. 4 ($T \sim 1800°$K).

If these pseudocylindrical waves observed in the laboratory were also detected in space, the measurement of their wavelength at different frequencies would help to reduce the uncertainty which still remains in the evaluation of the temperature of the ionospheric or magnetospheric plasma.

[1]R. K. Fisher and R. W. Gould, Phys. Fluids 14, 857 (1971).

[2]A. Gonfalone, J. Phys. (Paris) 33, 521 (1972).

[3]D. A. McPherson, J. H. Matsumoto, H. C. Koons, and W. B. Harbridge, "Resonance Cone in the Near-Field Pattern of a Satellite-Borne Electric Dipole Antenna" (to be published).

[4]I. B. Bernstein, Phys. Rev. 109, 10 (1958).

[5]T. H. Stix, The Theory of Plasma Waves (McGraw-Hill, New York, 1962).

[6]J. A. Tataronis and F. W. Crawford, J. Plasma Phys. 4, 249 (1970).

[7]J. Trulsen, J. Plasma Phys. 6, 367 (1971).

[8]H. Oya, J. Plasma Phys. 8, 183 (1972).

Normal Fluid Density, Second Sound, and Fourth Sound in an Anisotropic Superfluid

W. M. Saslow

Department of Physics, Texas A & M University, College Station, Texas 77843
(Received 5 July 1973)

In a superfluid with an anisotropic quasiparticle energy, the normal-fluid density is a diagonal tensor. The second and fourth sound velocities are distinctly anisotropic, so that heat-pulse or fourth-sound studies with an applied magnetic field $\vec{H}$ may permit identification of the direction of the gap axis with respect to $\vec{H}$. High-frequency sound velocities may display a weaker anisotropy.

I have studied the normal fluid density in an anisotropic superfluid, using Bardeen's[1] and Leggett's[2] generalizations of Landau's arguments for He II.[3] The results have been applied to second sound, fourth sound, and the determination of the energy gap near the transition temperature from a knowledge of the normal-fluid density. These questions are relevant because of the recent flurry of activity, both experimental and theoretical, prompted by the observations of Osheroff, Richardson, and Lee.[4]

It appears that, for $T \lesssim 3$ mK, and under pressure, liquid He^3 undergoes two phase transitions. It has been suggested that these involve superfluid states.[5,6] The higher-temperature phase, because of its unusual NMR resonance shift,[7] appears to be an anisotropic superfluid. The lower-temperature phase shows no such unusual magnetic behavior, but viscosity studies[8] indicate that it is in a superfluid state (presumably isotropic). We will employ the identification[9] of the higher-temperature phase as an AM (Anderson-Morel) state,[10] and the lower-temperature phase as a BW (Balian-Werthamer) state.[11] Recent heat-flow studies support a two-fluid model and have determined a phase diagram.[12]

In the absence of superflow, the momentum density of noninteracting fermion quasiparticles at temperature T is given by[1]

$$\vec{j} = V^{-1} \sum_{\vec{p}} \vec{p} f(\beta(E_p - \vec{p} \cdot \vec{v}_n))$$

$$= -\beta V^{-1} \sum_{\vec{p}} \vec{p} (\vec{p} \, \partial f/\partial x) \cdot \vec{v}_n + O(v_n^2); \tag{1}$$

$$f(x) = (e^x + 1)^{-1}. \tag{2}$$

Here V is the volume of the system, $\vec{p}$ is the momentum of a quasiparticle, E_p is its energy, $\beta = (K_B T)^{-1}$, and $\vec{v}_n$ is the normal-fluid velocity. Using $\vec{j} = \overleftrightarrow{\rho}_n^{(0)} \cdot \vec{v}_n$, one sees that

$$\overleftrightarrow{\rho}_n^{(0)} = -\beta V^{-1} \sum_p \vec{p} \, \vec{p} \, \partial f/\partial x. \tag{3}$$

Since $\overleftrightarrow{\rho}_n^{(0)}$ is real and symmetric, it can always be diagonalized. If the argument of f (i.e., βEp) is isotropic, then $\overleftrightarrow{\rho}_n^{(0)} = \rho_n^{(0)} \overleftrightarrow{1}$. However, if E_p is anisotropic $\overleftrightarrow{\rho}_n^{(0)}$ need not be proportional to the unit tensor $\overleftrightarrow{1}$. To be specific, we consider the model[10,13]

$$E_p = [\epsilon_p^2 + \Delta^2 \sin^2\theta_p]^{1/2}, \tag{4}$$

$$\epsilon_p \equiv p^2/2m^* - \epsilon_F.$$

Here, m^* is the effective mass of the quasiparticle, and ϵ_F is the Fermi energy, corresponding to the Fermi momentum p_0. θ_p is measured with respect to the gap axis. In this case the non-